Experimental Eye Research 206 (2021) 108518

Contents lists available at ScienceDirect

Experimental Eye Research

journal homepage: www.elsevier.com/locate/yexer

Echinomycin mitigates ocular angiogenesis by transcriptional inhibition of the hypoxia-inducible factor-1

Flavia Plastino [a,1], Álvaro Santana-Garrido [a,b,1], Noemi Anna Pesce [a], Monica Aronsson [a], Emma Lardner [a], Alfonso Mate [b], Anders Kvanta [a], Carmen Maria Vázquez [b], Helder André [a,*]

[a] Department of Clinical Neuroscience, Division of Eye and Vision, St. Erik Eye Hospital, Karolinska Institutet, Stockholm, Sweden
[b] Departamento de Fisiología, Facultad de Farmacia, Universidad de Sevilla, Seville, Spain

ARTICLE INFO

Keywords:
Age-related macular degeneration
Angiogenesis
Retina endothelium
Choroidal neovascularization
Echinomycin
Hypoxia-inducible factor

ABSTRACT

Background: Echinomycin (EKN), an inhibitor of hypoxia-inducible factor (HIF)-1 DNA-binding activity, has been implied as a possible therapeutic agent in ischemic diseases. Here, we assess EKN in hypoxia-driven responses *in vitro* using human primary adult retinal pigment epithelium cells (aRPE) and retinal endothelial cells (hREC), and *in vivo* using the laser-induced mouse choroidal neovascularization (CNV) model.

Methods: Effects of EKN on hypoxia-mediated pathways in aRPE were analyzed by Western blotting for HIF-1α protein, quantitative PCR of HIF-target genes, and proteome array for soluble angiogenic factors. *In vitro* inhibition of angiogenesis by EKN was determined in hREC. *In vivo* inhibition of angiogenesis by EKN was determined in the mouse laser-induced CNV, as a model of HIF-associated ocular neovascularization. CNV lesion area was determined by fundus fluorescein angiography.

Results: aRPE treated with EKN showed hypoxia-dependent significantly decreased cell recovery in the wound healing assay. These results were supported by lower levels of HIF-mediated transcripts detected in hypoxic aRPE cells treated with EKN compared with non-treated controls, and confirmed by proteome profiler for angiogenic factors. hREC exposed to aRPE EKN-conditioned medium displayed reduced sprouting angiogenesis. Mice with laser-induced CNV treated with intravitreally injected EKN showed significantly decreased vascular lesion area when compared with a mouse equivalent of aflibercept, or vehicle-treated controls.

Conclusions: Our data proposes EKN as a potent inhibitor of HIF-mediated angiogenesis in retinal cells and in the mouse model of CNV, which could have future implications in the treatment of patients with neovascular age-related macular degeneration.

1. Introduction

Age-related macular degeneration (AMD) is one of the leading causes of blindness in the elderly population of developed countries. An estimated 10% of late stage AMD patients are affected by the exudative or neovascular form of AMD (Mammadzada et al., 2020). Neovascular AMD (nAMD) is characterized by the progressive accumulation of drusen deposits between the retinal pigment epithelium (RPE) and the Bruch's membrane (Algvere et al., 2016; Miller, 2013). The presence of drusen reduces oxygen supply from the underlying choroid to the RPE. Lack of oxygen leads RPE cells into hypoxia (Arjamaa et al., 2017; Eltzschig and Carmeliet, 2011; Mammadzada et al., 2020; Vadlapatla et al., 2013). In response to hypoxia, the hypoxia-inducible factor-1 (HIF-1) mediates the transcription of several target genes (Ke and Costa, 2006; Ruas and Poellinger, 2005; Weidemann and Johnson, 2008), including the vascular endothelial growth factor (VEGF). VEGF is a key promoter of vascular leakage and neoangiogenesis, described as the formation of new blood vessels from the pre-existing (Semenza, 2011; Smith et al., 2020), and increased secretion of VEGF by the hypoxic RPE cells is considered one of the main underlying mechanism of choroidal neovascularization (CNV), a clinical condition associated with nAMD (Campochiaro, 2013; Kvanta, 2006, 2008).

HIF-1 is an heterodimeric transcription factor composed of an oxygen-dependent α-subunit (HIF-1α) and a constitutively expressed β-subunit (HIF-1β) (Semenza, 2007; Wang et al., 1995; Wang and Semenza, 1995). In normoxia, HIF-1α is degraded by the

* Corresponding author. St Erik Eye Hospital, Research, Eugeniavägen 12, 17164, Solna, Sweden.
E-mail address: Helder.Andre@ki.se (H. André).
[1] FP and ASG contributed equally to the work presented here and should therefore be regarded as equivalent authors.

https://doi.org/10.1016/j.exer.2021.108518
Received 29 October 2020; Received in revised form 29 January 2021; Accepted 15 February 2021
Available online 25 February 2021

ubiquitin-proteasome complex (Huang et al., 1998; Semenza, 2007; Weidemann and Johnson, 2008), while in hypoxia, HIF-1α translocates into the nucleus and heterodimerize with HIF-1β. HIF-1α/β complex recognizes specific DNA-binding sites, the hypoxia response elements (HRE), to activate the transcription of a series of HIF-1α target genes (Ke and Costa, 2006; Semenza, 2011). HIF-1α target genes are involved in a multitude of mechanisms that maintain homeostasis and ensure survival to oxygen deprivation, including glycolytic metabolism, apoptosis, cell proliferation, inflammation, angiogenesis, and formation of red blood cells, amongst others (Ke and Costa, 2006; Vadlapatla et al., 2013).

Anti-VEGF drugs are the primary form of treatment in ocular disease related to neovascular processes, including nAMD. Nonetheless, anti-VEGF drugs mainly target the vascular leakage, lose efficacy over time and repeated injections may pose some concerns on systemic safety (Daniel et al., 2020; Grunwald et al, 2015, 2017; Martin et al., 2012), which highlight the need for new forms of therapy for ocular neovascular diseases. Echinomycin (EKN) has been implied as a possible therapeutic agent in neovascular tumorigenesis (Kwon et al., 2011; Shin et al., 2011; Yao et al., 2017). EKN is a small peptide antibiotic that intercalates into the HRE sequences of HIF-1 target genes, resulting in direct inhibition of HIF-1 DNA-binding activity and subsequent reduction of hypoxia-mediated transcript levels, including VEGF (Kong et al., 2005; Kwon et al., 2011). Similarly to neovascular tumors, nAMD has been associated with upregulation of HIF-dependent mechanisms and progression of disease, both in patients (Inoue et al., 2007; Sheridan et al., 2009) and in animal models (André et al., 2015; Lin et al., 2012). The mechanism of action of EKN compared to anti-VEGFs may avoid the disadvantages of anti-VEGF therapies, by inhibiting multiple proangiogenic factor simultaneously.

EKN has not been studied thus far in eye tissues. The aim of the present study is to determine the role of EKN in hypoxia-driven ocular responses both *in vitro* using human primary adult retinal cells and *in vivo* using an animal model of CNV.

2. Material and methods

2.1. Cell culture and treatments

Human adult retinal pigment epithelium (aRPE) cells (Innoprot, Derio, Spain) were cultured to confluence in DMEM/F12 medium (1:1 mixture Dulbecco's Modified Essential Medium and Ham's F-12 Medium; ThermoFisher Scientific Inc., Waltham, MA, USA), supplemented with 1% penicillin-streptomycin antibiotics (P/S; ThermoFisher Scientific Inc.) and 10% fetal bovine serum (FBS; ThermoFisher Scientific Inc.). Human retinal endothelial cells (hREC; Innoprot) were cultured to confluence in endothelial cell growth base media with endothelial cell growth supplement (R&D Systems, Abingdon, UK). aRPE and hREC were kept at normoxia in a standard cell culture incubator (20% oxygen, 5% carbon dioxide at 37 °C).

aRPE were exposed to hypoxia (1% oxygen, 5% carbon dioxide at 37 °C), in presence or absence of EKN according to experimental protocols.

EKN (CAS number: 512-64-1: Tocris, Abingdon, UK) was dissolved in dimethyl sulfoxide (DMSO; Sigma-Aldrich Corp., St. Louis, MO, USA) at 5 mM and subsequently diluted to 5pM in Ham's F-12 medium, supplemented with 1% FBS, 1% P/S and 1x HEPES (ThermoFisher Scientific Inc.).

2.2. Wound healing assay

aRPE monolayers were cultured in 6-well plates and mechanically scratched with a plastic 100 μL pipette tip, in a cross pattern. The cultures were kept in normoxia conditions or exposed to hypoxia in the presence or absence of EKN as designated. Wound healing process was tracked through time and phase-contrast images of wounded areas were acquired every 12 h (PrimoVert; Zeiss, Gottingen, Germany). The measurements of the wounded area at each time point were performed using ImageJ software, as average of the wound diagonals.

2.3. In vitro angiogenesis assay

hREC were cultured for 24 h in endothelial cell growth base media supplemented with 1% P/S and 0.4% methylcellulose (Sigma-Aldrich Corp.) to form spheroids (1000 cells), which were subsequently transferred to flat-bottom adherent 96-well plates, previously coated with geltrex extracellular matrix (ThermoFisher Scientific Inc.) and incubated at 37 °C for 1 h. To perform a sprouting assay, spheroids were exposed for 48 h to aRPE conditioned media as described in human angiogenesis array. The angiotool software (Zudaire et al., 2011) was used to analyze the 3D cultures in regard to total branching index, total branching area, number of endpoints, and number of junctions; referred as vasculature, vasculature area, sprouts, and branching, respectively.

2.4. Human angiogenesis array

aRPE cells were cultured in Ham's F-12 media supplemented with 1% P/S, 1% FBS and 1x HEPES, and exposed to 24 h of hypoxia with or without EKN. Conditioned media from normoxia (used as control), hypoxia, and hypoxia treated with EKN were collected to analyze soluble proteins. The proteome profiler human angiogenesis array (cat. no. ARY007; R&D Systems) was used to analyze expression of 55 angiogenesis-related proteins simultaneously. The blots were developed and scanned, and the differences in protein expression were determined by densitometric analysis corrected with the three positive controls, as recommended by the manufacturer.

2.5. Animals and CNV induction

All animals were used in accordance with the ARVO statement for the use of animals in ophthalmologic and vision research, and the study protocols were approved by Stockholm's committee for ethical animal research. A total of 54 C56BL/6 J mice were kept with a 12 h day/night cycle, free access to food and water and monitored daily. Mice were euthanized by cervical dislocation, as approved by the ethical committee. 8-week-old mice were anesthetized as described (Takei et al., 2017). CNV lesions were induced with the laser-coupled micron IV (Phoenix Research Labs, Pleasanton, CA, USA) set for 50 μm spot, 180 mW intensity, 100 ms duration.

2.6. Pharmacological treatments

Animal were randomly distributed into three groups and both eyes were intravitreally injected with two administrations of 1 μL of vehicle (PBS), 1 μg/μL of recombinant mouse VEGFR1-Fc chimera protein (a mouse aflibercept equivalent; R&D Systems), or 1 μg/μL EKN on both days 3 and 6 after laser induction. CNV lesion area was determined on day 9 post-laser by fundus fluorescein angiography (FFA). Briefly, anesthetized mice were injected subcutaneously with 30 mg/kg of a 10% fluorescein sterile solution (Alcon Nordic, Copenhagen, Denmark) and imaged with fixed camera exposure settings, 5 min after injection. Exclusion criteria of CNV laser spots followed the recommended outliers, as previously described (Lambert et al., 2013). At day 9 post-laser mice were euthanized and the eyes enucleated. The RPE/choroids complex from each eye were dissected and frozen in liquid nitrogen prior to molecular analysis (André et al., 2015).

2.7. Histological stainings

Mice intravitreally injected with 1 pg, 1 ng, 1 μg and 10 μg of EKN in 1 μL on days 0 and 3. On day 9, mice were euthanized and eyeballs enucleated, fixed for 24 h, and subsequently processed for paraffin embedding and sectioning. 4 μm sections of mouse retinas were

processed for hematoxylin and eosin or immunohistofluorescence staining in a Bond III robotic system (Leica Biosystems, Newcastle, UK), as previously described (André et al., 2015). Sections were incubated with primary antibody: anti-IBA1 (1:100, rabbit monoclonal, cat. no. ab178846; Abcam, Cambridge, UK) and GFAP (1:1.000, rabbit monoclonal, cat. no. ab68428; Abcam). Secondary antibody incubations were performed with anti-rabbit-Alexa 546 (1:500, goat polyclonal, cat. no. A11010; ThermoFisher Scientific Inc.) and Hoechst 33,258 (Sigma-Aldrich Corp.). Sections were mounted with fluorescence mounting medium (Dako, Carpinteria, CA, USA), and visualized with an Axioscope 2 plus with the AxioVision software (Zeiss, Gottingen, Germany).

2.8. Western blot

Whole-cell extracts (WCE) were prepared in RIPA lysis buffer (Sigma-Aldrich Corp.) while mouse RPE/choroid complex whole-tissue extracts (WTE) were prepared with a SingleShot lysis kit (BioRad Laboratories, Hercules, CA, USA). 15 μg of total protein from WCE or WTE were separated by SDS-PAGE electrophoresis and transferred on polyvinylidene difluoride (PVDF) membranes (BioRad Laboratories). Blots were blocked using 5% non-fat milk in Tris-buffered saline (nfm/TBS; 20 mM Tris, 500 nM NaCl, pH 7,4; BioRad Laboratories). Subsequently, membranes were incubated with primary antibodies: anti-actin (1:10.000, rabbit monoclonal, cat. no. SAB5600204; Sigma-Aldrich Corp.); anti–HIF–1α (1:500, rabbit polyclonal, cat. no. NB100479; Novus Biologicals, Abingdon, UK); anti-VEGF (1:200, mouse monoclonal, cat.no. SAB4200815; Sigma-Aldrich Corp.) for 1 h at room temperature (RT). Secondary antibodies anti-rabbit-IgG (cat. no. P044801-2) or anti-mouse-IgG (cat. no. P044701-2) conjugated to horseradish peroxidase (1:10.000; Dako) were used for 1 h at RT. Both antibodies steps were performed in 1% nfm in TBS-T (TBS supplemented with 0.05% Tween-20; Sigma-Aldrich Corp.), followed by extensive TBS-T washes. Protein signals were detected by enhanced chemiluminescence (ECL; ThermoFisher Scientific Inc.) on a Chemidoc MP imaging system (BioRad Laboratories). Protein levels were determined by densitometry analysis using the ImageJ (NIH freeware) and corrected to the actin loading control.

2.9. Quantitative PCR

Total RNA was extracted from aRPE cells at 95% confluence using RNeasy mini kit (Qiagen, Hilden, Germany) according to the manufacturer's instruction. Mouse RPE/choroid complexes total RNA was extracted with a SingleShot lysis kit (BioRad Laboratories). cDNA was produced from 1 μg total RNA using iScript first strand kit (BioRad Laboratories). iQSYBR green supermix and primer pair oligos were used to determine transcripts expression, in a CFX96 thermal cycler (all BioRad Laboratories). Certified PrimePCR oligos included: HIF-1α (cat. no qMmuCIP0030996); phosphoglycerate kinase 1 (PGK1; cat. no. qHsaCED0042912); erythropoietin (EPO; cat. no. qHsaCED0004712); carbonic anhydrase 9 (CA9; cat. no. qHsaCID0017667); VEGF (cat. no. qHsaCED0006937 and qMmuCED0040260); VEGF receptor 1 (VEGFR1; cat. no. qHsaCEP0050201); insulin-like growth factor 2 (IGF2; cat. no. qHsaCED0046446); insulin-like growth factor binding protein 3 (IGFBP3; cat. no. qHsaCID0010824); matrix metalloproteinase 2 (MMP2; cat. no. qHsaCID0015623); plasminogen activator inhibitor 1 (PAI-1; cat. no. qHsaCID0006432); urokinase-type plasminogen activator (uPA; cat. no. qHsaCID0019740). Threshold values were analyzed by the ΔΔCt method and data were determined relative to two housekeep genes: TATA-box binding protein (TBP), cat. no. qHsaCID0007122 and qMmuCID0040542; hypoxanthine phosphoribosyltransferase 1 (HPRT1), cat. no. qHsaCID0016375 and qMmuCID0005679.

2.10. Statistical analysis

Statistical significance was determined by one-way ANOVA, followed by Newman-Keuls multiple comparison posttest using the GraphPad software (San Diego, CA, USA). The results were expressed as mean ± standard error of mean of the indicated n values. Differences with $P < 0.05$ were considered statistically significant.

3. Results

3.1. EKN reduces HIF-1α–dependent wound healing recovery in RPE in vitro

aRPE cells were treated with 0, 5 or 50 pM of EKN, and exposed to 24 h of hypoxia or kept at normoxia as control. Western blot analysis was performed to determine the effect of EKN on HIF-1α protein levels and establish the optimal concentration for subsequent studies (Fig. 1A). Densitometric analysis demonstrated that 0 and 5 pM of EKN had no effects on HIF-1α at protein level, in both normoxia and hypoxia. Concentrations of 50 pM of EKN caused a significant reduction of HIF-1α protein expression ($P < 0.001$), as compared to hypoxia levels (Fig. 1B). These results were confirmed by an *in vitro* wound healing assay, which further characterized the effects of EKN on HIF-1α–dependent mechanisms of aRPE cells migration and/or proliferation, as characteristic of this method. aRPE cells treated with 50 pM of EKN showed an inhibition of wounded area recovery, in both normoxia and hypoxia (Fig. 2A). A statistically significant inhibition of wounded area recovery was observed in aRPE cells treated with 5 pM EKN ($P < 0.001$), under hypoxic conditions (Fig. 2B). This data suggested that 50 pM or higher concentrations of EKN may interfere with HIF-1α–independent mechanisms, thus implying toxic effects on aRPE cells. In line with the present findings, subsequent *in vitro* experiments were performed with 5 pM EKN concentrations.

3.2. EKN inhibits HIF-1α–mediated responses in hypoxic aRPE cells

To analyze the effect of EKN on HIF-1α transcriptional activity, a series of canonical HIF-1α–mediated genes involved in hypoxia, angiogenesis, cell survival, and migration were analyzed by qPCR in aRPE cells exposed to hypoxia, in the presence or absence of 5 pM of EKN (Fig. 3). Data analysis revealed a statistically significant increase of transcript levels in response to hypoxia, including PGK1 and PAI-1 ($P < 0.05$), CA9 ($P < 0.01$), VEGF and IGFBP3 ($P < 0.001$). Contrastingly,

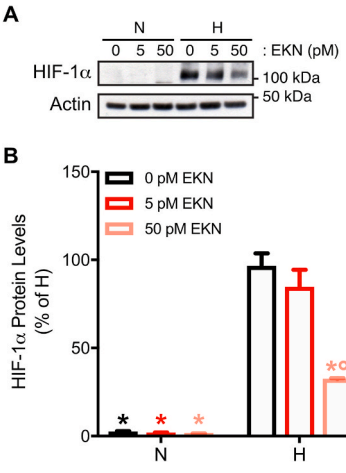

Fig. 1. Effects of EKN on HIF-1α protein level in aRPE cells. (**A**) Western blot analysis of HIF-1α in aRPE cells treated with 0, 5, or 50 pM of EKN under normoxia (N) or hypoxia (H), showed no effects of EKN on HIF-1α at protein levels at concentration of 5 pM. (**B**) Densitometric analysis displayed a non-significant reduction of HIF-1α with 5 pM of EKN, while significant with 50 pM of EKN. Data were corrected versus the actin loading control, and presented as percentage of H ($n = 3$). $P < 0.05$: * vs H; ° vs 5 pM EKN.

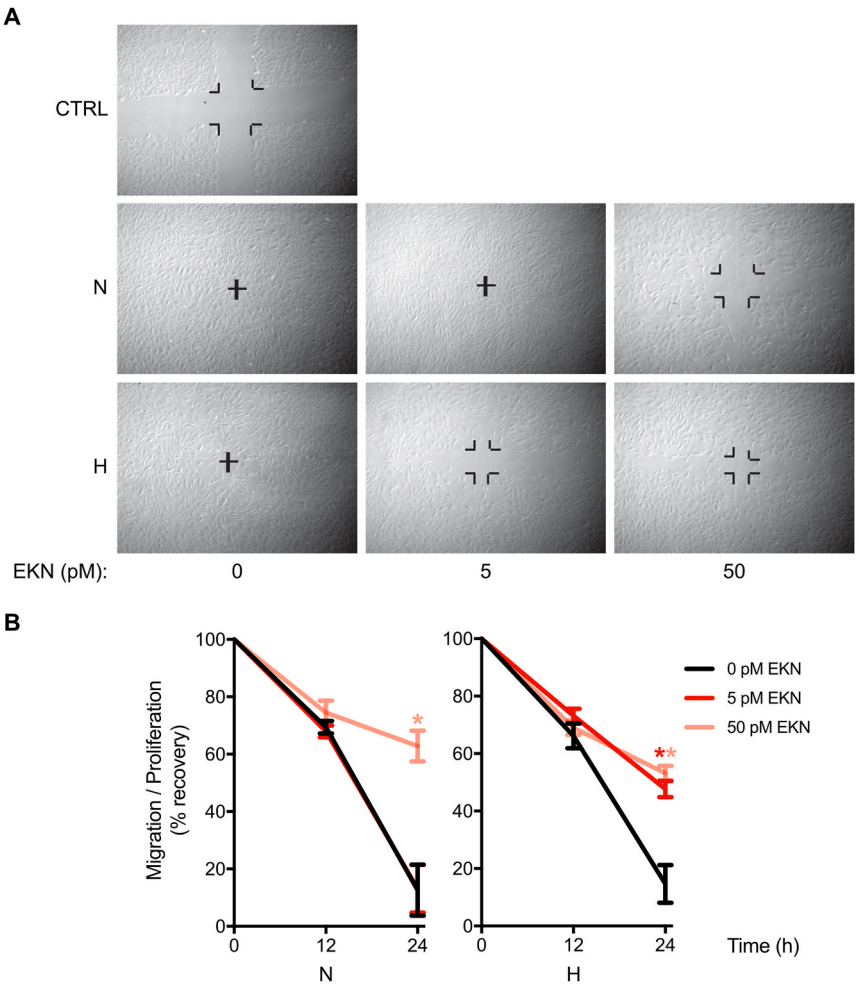

Fig. 2. Effects of EKN on aRPE cell wound healing. (**A**) *In vitro* wound healing assay was performed in monolayers of aRPE cells treated with 5 or 50 pM of EKN, under normoxia (N) or hypoxia (H). (**B**) Quantitative analysis revealed a significant reduction in migration with 5 pM of EKN under H, unlike in N. A significant reduction in wounded area recovery with 50 pM of EKN was determined both in N and H. Data were presented as a percentage of recovery ($n = 5$). $P < 0.05$: * vs N or H.

hypoxic aRPE cells treated with EKN demonstrated a statistically significant decrease of PGK1 ($P < 0.05$), CA9 and PAI-1 ($P < 0.01$), VEGF and IGFBP3 ($P < 0.001$) transcript levels, when compared to hypoxia. However, transcript levels of hypoxia-mediated genes such as EPO, VEGFR1, IGF2, MMP2, and uPA did not statistically differ in aRPE cells under hypoxic conditions nor in response to EKN.

Proteome profiler analysis was used to determine the expression of soluble factors involved in angiogenesis, cell survival, migration and chemotaxis, using conditioned media from aRPE cells exposed to 24 h of hypoxia in the presence or absence of 5 pM of EKN (Fig. 4A). Densitometric analysis illustrated a general increase of VEGF ($P < 0.001$), thrombospondin 1 (TSP-1; $P < 0.001$), IGFBP2 ($P < 0.05$), IGFBP3 ($P < 0.001$), pigment epithelium-derived factor (PEDF; $P < 0.01$), pentraxin-related protein 3 (PTX3; $P < 0.05$), metalloproteinase inhibitor 1 (TIMP-1; $P < 0.01$), C-X-C motif chemokine ligand 16 (CXCL16; $P < 0.001$) in response to hypoxia (Fig. 4B). Upon treatment with 5 pM EKN protein

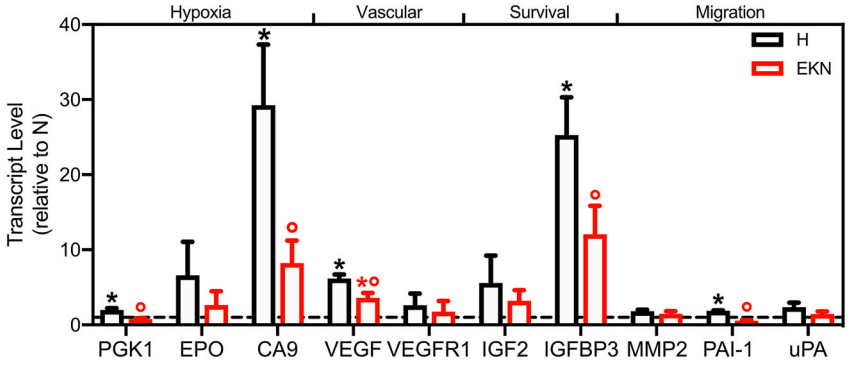

Fig. 3. EKN acts on HIF-1α transcriptional activity in hypoxic aRPE cells. qPCR analysis of HIF-1α–mediated genes involved in hypoxia, angiogenesis, cell survival, and migration was performed in aRPE cells exposed to hypoxia (H) in the presence or absence of 5 pM EKN. Data demonstrated a significant decrease of CA9, VEGF and IGFBP3 transcript levels in the presence of EKN, after an increase in response to H. Data were normalized by the ΔΔCt method relative to normoxia (N; $n = 5$). $P < 0.05$: * vs N; ° vs H.

levels of PTX3 ($P < 0.05$), TSP-1, PEDF, TIMP-1 ($P < 0.01$), and VEGF, IGFBP3, CXCL16 ($P < 0.001$) decreased significantly, as compared to hypoxic levels. Of relevance, IGFBP2 protein secretion levels were not reduced by EKN treatment, while soluble VEGF was decreased to levels significantly lower than the normoxic controls ($P < 0.01$).

3.3. EKN mitigates angiogenesis in hREC

To evaluate the role of EKN in angiogenesis, 3D spheroid cultures of hREC were used to induce angiogenic sprouting when embedded in extracellular matrixes (Fig. 5A). A significant increase of vasculature, vasculature area, sprouts and branching were observed in spheroids exposed to hypoxic-conditioned aRPE cell media (all $P < 0.001$), compared to spheroid cultures exposed to normoxia-conditioned aRPE media (Fig. 5B). Exposure of 3D spheroid cultures to hypoxic EKN-treated aRPE cells media significantly reduced the assessed vascular parameters to levels comparable to normoxic controls (all $P < 0.001$ versus hypoxia). The results implied that 5pM of EKN mitigates retinal *in vitro* angiogenesis through a reduction of HIF-1α–dependent transcriptional activity in RPE cells.

3.4. EKN mitigates in vivo choroidal neovascularization

To further investigate the role of EKN in ocular angiogenesis, *in vivo* studies were performed in mouse eyes. First, a dose escalation and toxicology analysis were determined to better characterize the optimal ocular concentration of EKN for subsequent experiments (Fig. 6). The histopathological analyses of retinal sections from mice treated with intravitreal injections of 1 pg, 1 ng, 1 μg and 10 μg of EKN per eye revealed that doses lower than 10 μg showed no differences compared to vehicle. However, 10 μg of EKN intravitreally led to cell infiltrations both in proximity to the ganglion cells layer and the RPE layer. Moreover, immunohistofluorescence analysis indicated the presence of glyotic and inflammatory responses in retinas exposed to 10 μg of EKN, as determined by the increased presence of GFAP-positive Müller glia and IBA1-positive microglia cells as compared to lower doses of EKN. These results imply that 10 μg of intravitreal EKN could lead to toxic events in mouse retinas, and subsequent *in vivo* experiments were conducted at 1 μg/μL by intravitreal administration of EKN.

As previously demonstrated, laser-induced CNV mice undergo HIF-1α–dependent angiogenesis (André et al., 2015). In this study, laser-induced CNV mice were intravitreally treated with two administration (days 3 and 6 post-laser induction) of 1 μL of vehicle, or 1 μg/μL of EKN or VEGFR1-Fc chimera (a mouse equivalent of aflibercept), with non-lasered mice as controls (Fig. 7A). CNV lesion was analyzed by FFA imaging on day 9 post-laser, correlating to the peak of HIF-1α–associated events in this model (André et al., 2015). Fundus images demonstrated a statistically significant CNV reduction in eyes treated with EKN compared with vehicle and VEGFR1-Fc chimera (both $P < 0.001$). Of relevance, the quantitative percentage of reduction for VEGFR1-Fc chimera-treated eyes was 76.76 ± 5.07%, while eyes treated with EKN showed a reduction of 29.53 ± 15.38% in CNV lesion area, as compared with the vehicle-treated group.

Further analyses were performed to investigate the effect of EKN on HIF-1α and VEGF expression both at transcript (Fig. 7B) and protein (Fig. 7C) levels. Despite no changes in HIF-1α transcript levels, protein expression was upregulated in response to laser-induced CNV ($P < 0.05$) and was independent of treatments with either VEGFR1-Fc chimera or EKN. VEGF transcript and protein levels were significantly increased in CNV-induced eyes ($P < 0.05$ and $P < 0.001$, respectively), as compared to non-treated controls. CNV eyes treated with EKN demonstrated statistically significant reduction of VEGF transcript ($P < 0.001$ versus both vehicle and VEGFR1-Fc chimera) and protein ($P < 0.001$ versus vehicle) expression, to levels compared with the non-treated control group. In addition, VEGFR1-Fc chimera-treated CNV eyes displayed a significant decrease only in VEGF protein levels ($P < 0.001$ versus vehicle). Collectively, these data suggested that EKN mitigates angiogenesis in the laser-induced CNV by inhibiting the HIF-associated increase of VEGF in this mouse model.

4. Discussion

AMD is one of the leading causes of blindness worldwide, with increasing prevalence interrelated to an aging population (Lindekleiv and Erke, 2013; Wong et al., 2014). The neovascular form of AMD has gained considerable attention amongst neovascular diseases, mainly

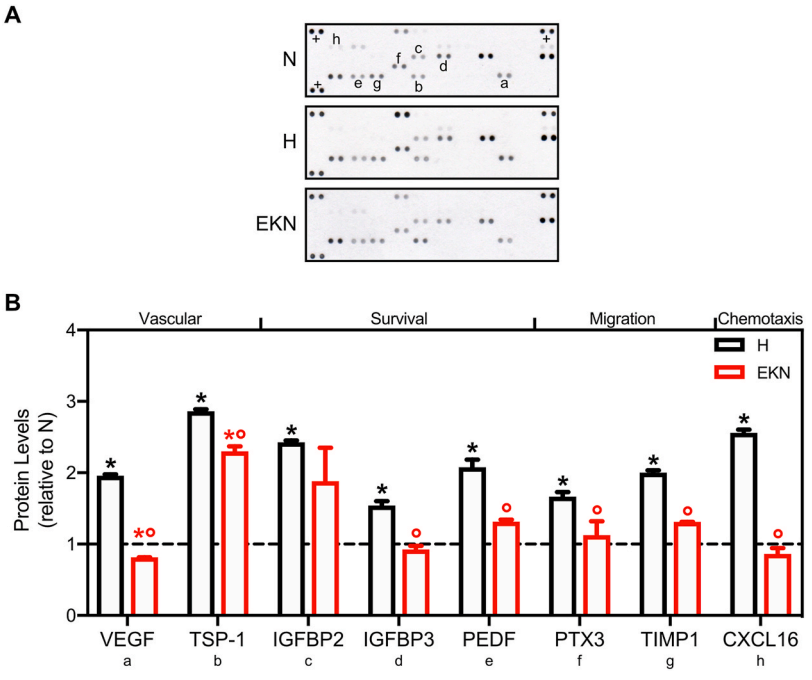

Fig. 4. Soluble factors expression profile from aRPE cells in response to hypoxia and EKN. (**A**) Conditioned media from aRPE cultures exposed to 24 h of normoxia (N), or hypoxia (H) and treated with 5 pM EKN were analyzed by proteome profiler. (**B**) Densitometric analysis showed a general increase of soluble factors involved in vascular responses, cell survival, migration, and chemotaxis in hypoxic aRPE cells, with concomitant decrease when treated with EKN. Data were corrected to the average of internal positive controls (+) and normalized to N ($n = 3$). $P < 0.05$: * vs N; ° vs H.

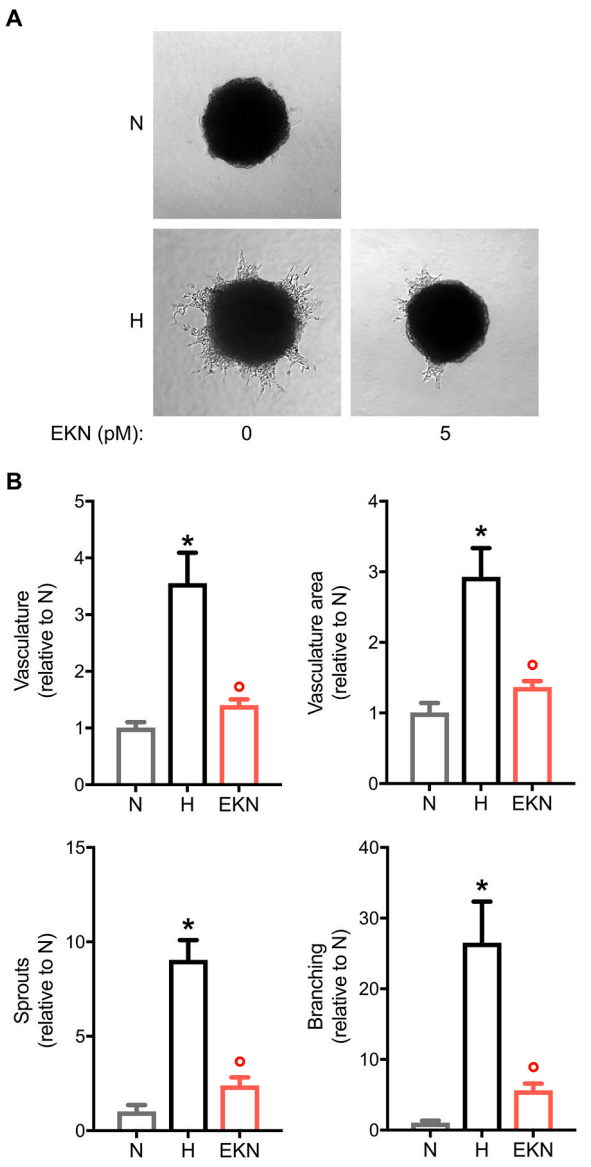

Fig. 5. EKN-conditioned aRPE media inhibits angiogenesis in hREC. (**A**) Sprouting assay was performed in hREC spheroids exposed to hypoxic EKN-treated aRPE medium. (**B**) Quantitative analysis illustrated a significant reduction in the analyzed vascular parameters in spheroids exposed to EKN-treated medium. Data are presented as fold versus N ($n = 9$). $P < 0.05$: * vs N; ° vs H.

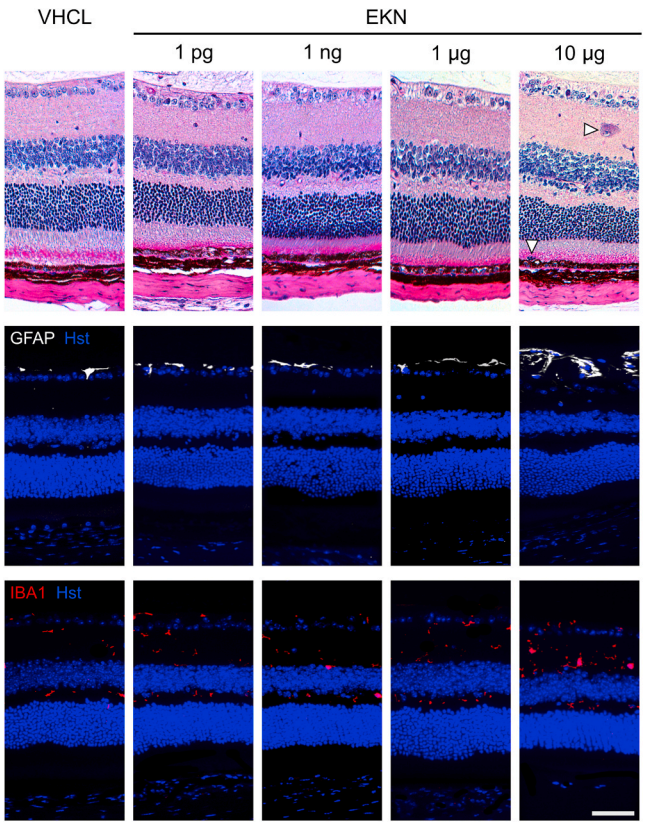

Fig. 6. Dose escalation and toxicology of EKN in mouse retina. Hematoxylin and eosin stained sections of retinas treated with intravitreal EKN were compared to vehicle (VHCL). Increasing doses of EKN suggested that 10 µg/µL of intravitreal EKN ($n = 4$ per dose) led to infiltrating cells into the retina (arrow heads), a sign of putative toxic events. Immunohistofluorescence with nuclear counterstain (Hst; blue) of retinas treated with 10 µg/µL of EKN confirmed an increase in GFAP-positive Müller glial cells (white) and IBA1-positive microglia cells (red). Scale bar = 50 µm.

with the discovery of anti-VEGF drugs in ophthalmology (Miller, 2013). Nevertheless, anti-VEGF treatments must be repeated often with elevated costs for health care systems and, with disease progression, loss of efficacy and significant incidence of associated geographic atrophy of the RPE (Daniel et al., 2020; Grunwald et al., 2015), to which there is no current treatment. These underline a need for assessing new therapies for nAMD, where HIF-mediated VEGF plays a pivotal role in the neo-angiogenic processes of the disease (André et al., 2015; Inoue et al., 2007; Lin et al., 2012; Sheridan et al., 2009). Previous studies have revealed that EKN suppresses VEGF (Kong et al., 2005; Kwon et al., 2011), advocating HIF-1α as an upstream target for anti-angiogenic treatment. The present study demonstrates for the first time the efficacy of EKN as an inhibitor of HIF-1α activity in ocular angiogenesis, both *in vitro* and *in vivo*.

EKN had not been tested in RPE cells previously. In the present study, different concentrations are assessed in hypoxic aRPE cells *in vitro*. Protein expression of HIF-1α in EKN-treated cells is undistinguishable from untreated controls at concentrations of 5pM of EKN. Wound healing assay demonstrates a reduction on migration and/or proliferation in aRPE cells with the same EKN concentration, as compared to hypoxic conditions. These findings are in agreement with the mechanism of action of EKN on HIF-1α at the DNA binding level (Kong et al., 2005). On the other hand, doses above 50 pM of EKN inhibit wound healing ability and alter HIF-1α protein levels, not only under hypoxia but also in normoxia, suggesting side-effects independent of HIF-1α pathways in aRPE cells. An *in vitro* study on adipogenesis identified HIF-independent mechanisms for high doses of EKN (Yamaguchi et al., 2017), thus suggesting that the method in the present study to identify low and effective doses for EKN in RPE cells benefits both to avoid toxic effects and eventual HIF-independent actions of EKN.

The effect of EKN on downregulation of the HIF-1α pathway can be determined by transcriptional modulation and soluble factors expression of HIF-1α–induced genes in aRPE cells. EKN treatment reduces vascular, survival, migration and chemotaxis HIF-mediated transcripts and proteins, compared to hypoxia controls. Particularly, VEGF is downregulated at both transcriptional and protein level in aRPE cells treated with EKN. The efficacy of EKN as a VEGF inhibitor through HIF-1α has been corroborated in human ectopic endometriotic stromal cells and hepatocytes, where EKN affects the expression of VEGF genes and reduces cell proliferation (McCullough et al., 2013; Tsuzuki et al., 2016). Despite VEGF pivotal role in ocular pathologies associated with CNV, multiple other neovascular factors have been reported to be upregulated

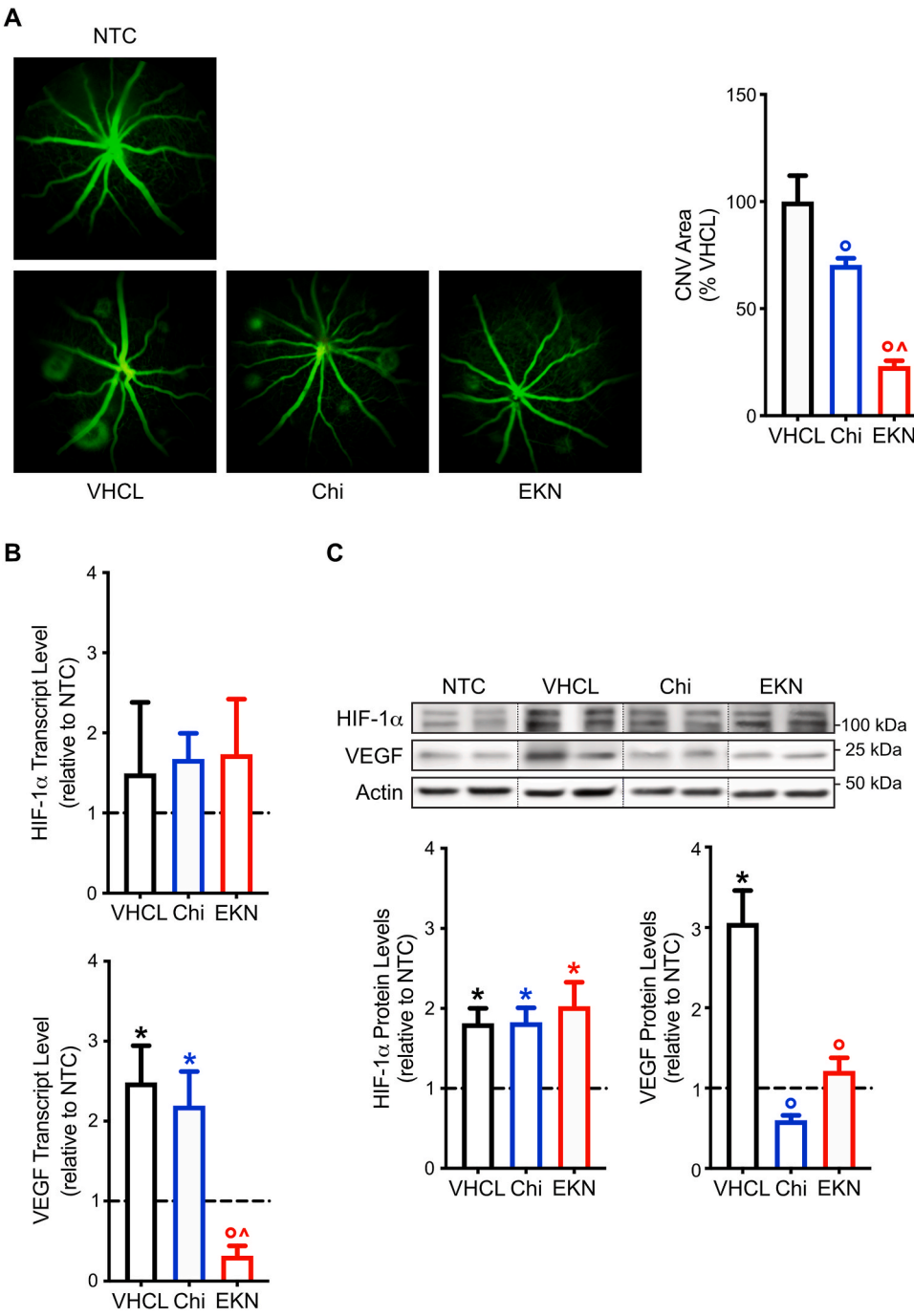

Fig. 7. Effects of EKN on the laser-induced CNV mouse model of nAMD. (**A**) FFA images of laser-induced mice on day 9 post-laser, following intravitreal injections of 1 μL vehicle (VHCL), 1 μg/μL of VEGFR1-Fc chimera (Chi), or 1 μg/μL of EKN, and compared to non-treated controls (NTC). Eyes treated with EKN showed a significant reduction of CNV lesion area, when compared to both VHCL- and Chi-treated eyes. Data are presented as percentage of VHCL ($n = 12$ spots per group). Molecular analysis of laser-induced CNV RPE/choroids complexes was performed by qPCR (**B**) and Western blot (**C**). EKN-treated eyes demonstrated a reduction of both transcript and protein levels of VEGF. qPCR data were normalized by the ΔΔCt method relative to NTC (dashed line; $n = 10$ eyes per group). Protein analysis is depicted by representative western blots and quantified by densitometry relative to NTC (dashed line; $n = 10$ eyes per group). $P < 0.05$: * vs NTC; ° vs VHCL; ^ vs Chi.

and mediated by HIF-1α in RPE cells (Arjamaa et al., 2017; Forooghian and Das, 2007; Kvanta et al., 1996; Takei et al., 2017). In addition to VEGF, EKN treatment of aRPE cells reduces hypoxia levels of a myriad of factors associated with nAMD (Vadlapatla et al., 2013), including IGFBP3, PAI-1, PEDF, PTX3, TIMP-1, CXCL16, and the canonical HIF-1α targets PGK1 and CA9. Collectively, these data suggest EKN as an effective *in vitro* regulator of ocular angiogenesis mediated by HIF-1α in aRPE cells. To support the *in vitro* efficacy of EKN on ocular angiogenesis, a sprouting assay was performed in retinal endothelial organoids exposed to EKN-treated RPE cells conditioned medium. Hypoxia aRPE cells condition medium increases the neoangiogenic sprouting in hREC, while EKN treatment reduces hREC sprouting neoangiogenesis to levels compared to normoxic controls. Taken together, the present *in vitro* data demonstrate that EKN can mitigate ocular HIF-mediated angiogenesis by downregulation of transcripts and proteins associated with neovascular events in RPE cells and able to crosstalk to retina endothelia, implying EKN as a possibly therapeutic candidate for nAMD, or even other retinal vascular diseases associated with hypoxia, such as retinopathy of prematurity (ROP) and central retinal vein occlusion (CRVO) (Kvanta, 2006; Mammadzada et al., 2016).

Hypoxia plays a pivotal role in nAMD through neoangiogenesis associated with HIF-1α, and consequently VEGF (Campochiaro, 2013; Kvanta, 2008; Mammadzada et al., 2020; Vadlapatla et al., 2013). In addition, the mouse model of laser-induced CNV has been associated with HIF-mediated RPE induction of VEGF (André et al., 2015; Lin et al., 2012), proposing the model as an ideal candidate to assess the efficacy of

EKN in reducing ocular neoangiogenesis *in vivo*. Similarly to the present *in vitro* paradigm, EKN is assessed for the first time in ocular tissues, thus a dose selection and toxicology analysis is performed on mice treated intravitreally with EKN. At higher doses (10 μg/μL intravitreal EKN) histopathological alteration of the RPE cells are observed and accompanied with infiltrating Müller glia and microglia cells into the retina. Doses of EKN lower than 1 μg/μL are deemed safe, without discernible alteration to retinal and choroidal histological structures. In addition, FFA images of laser-induced mice did not show any discernible signs related to toxicity, supporting the safety of the selected EKN dose for intravitreal administration. Doses of 1 μg/μL by intravitreal administration of EKN are in parallel with anti-VEGF drugs concentrations for ocular neovascular mouse models (Cammalleri et al., 2016; Locri et al., 2019), thus allowing equative comparison of EKN with anti-VEGF treatments in the mouse model of induced CNV. Laser-induced CNV lesion area is significantly reduced by EKN treatment, as well as by anti-VEGF treatment. Comparatively, the mouse VEGFR1-Fc chimera equivalent of aflibercept is less efficient in reducing CNV lesion area versus EKN, in the present experimental paradigm. These findings are corroborated with a reduction of VEGF protein levels by anti-VEGF treatment, which is not accompanied by reduction of VEGF transcripts in the mouse model of nAMD. Despite anti-VEGF therapies improving visual symptoms of nAMD patients, a number of treated eyes demonstrate ongoing negative effects such as geographic atrophy, fibrotic scarring or CNV leakage (Daniel et al., 2020; Grunwald et al, 2015, 2017), in addition to some patients not responding to anti-VEGF drugs (Nagai et al., 2016; Otsuji et al., 2013). The multifactorial etiology of nAMD could be the rationale for some of the observed anti-VEGF short-comings, since these treatments address a mono-factor strategy at the protein level alone. Molecular analysis of HIF-1α expression patterns demonstrates an unaltered transcript with increase in protein levels associated with CNV, in agreement with previous studies (André et al., 2015; Lin et al., 2012; Semenza, 2011). In addition, CNV eyes treated with EKN demonstrate reduction of HIF-mediated VEGF transcript and protein levels, unlike anti-VEGF treatments that do not reduce VEGF gene expression. Targeting CNV upstream of VEGF, by inhibition of HIF-1α by EKN, may result in downregulation of multiple neovascular factors associated with nAMD, as indicated here with VEGF. Albeit, the present study lacks in identifying multiple specific molecular effectors of EKN treatment in reducing CNV *in vivo*. Nonetheless, a previous study specifically targeting HIF downregulation in the mouse model of laser-induced CNV has demonstrated mitigation of nAMD-related neovascular factors (Takei et al., 2017), including HIF-1α genes related to angiogenesis (VEGF and IGFBP3), involved in chemotaxis (CXCL16 receptor; CXCR4), endothelial cell migration (PAI-1), and mandatory HIF-1α genes (PGK-1 and CA9). These findings are in synchrony with the present *in vitro* data, which imply that EKN could be downregulating the same families of factors *in vivo* as identified here *in vitro,* in addition to the presented for VEGF.

In sum, both *in vivo* and *in vitro*, the present study presents first evidence for the efficacy of EKN on mitigating ocular HIF-1α–mediated neoangiogenesis. These findings demonstrate the efficiency of therapeutic approaches towards exogenous control of endogenous gene expression as novel therapies for ocular pathologies associated with angiogenesis, such as AMD and putatively ROP and CRVO, and HIF-1α as a new target for these ocular diseases.

Funding

Supported by grants from The Crown Princess Margareta Association for the Visually Impaired (Valdemarsvik, Sweden), Karolinska Institutet Foundations (Stockholm, Sweden), The Swedish Eye Foundation (Umeå, Sweden), the Practicas Erasmus+ mobility program from the University of Seville (ASG; Seville, Spain), and the FPU predoctoral fellowship from *Ministerio de Ciencia, Innovación y Universidades* of the Spanish Government (ASG; FPU17/03465; Madrid, Spain).

Declaration of competing interest

The authors declare no conflicts of interest.

Acknowledgments

The authors thank Filippo Locri for technical support, Diana Rydholm for animal husbandry, and the histology laboratory at St Erik Eye Hospital for expertise in histopathology.

References

Algvere, P.V., Kvanta, A., Seregard, S., 2016. Drusen maculopathy: a risk factor for visual deterioration. Acta Ophthalmol. 94, 427–433. https://doi.org/10.1111/aos.13011.

André, H., Tunik, S., Aronsson, M., Kvanta, A., 2015. Hypoxia-inducible factor-1α Is associated with sprouting angiogenesis in the murine laser-induced Choroidal neovascularization model. Investig. Ophthalmol. Vis. Sci. 56, 6591–6604. https://doi.org/10.1167/iovs.15-16476.

Arjamaa, O., Aaltonen, V., Piippo, N., Csont, T., Petrovski, G., Kaarniranta, K., Kauppinen, A., 2017. Hypoxia and inflammation in the release of VEGF and interleukins from human retinal pigment epithelial cells. Graefe's Arch. Clin. Exp. Ophthalmol. 255, 1757–1762. https://doi.org/10.1007/s00417-017-3711-0.

Cammalleri, M., Dal Monte, M., Locri, F., Lista, L., Aronsson, M., Kvanta, A., Rusciano, D., De Rosa, M., Pavone, V., André, H., Bagnoli, P., 2016. The urokinase receptor-derived peptide UPARANT mitigates angiogenesis in a mouse model of laser-induced choroidal neovascularization. Investig. Ophthalmol. Vis. Sci. 57, 2600–2611. https://doi.org/10.1167/iovs.15-18758.

Campochiaro, P.A., 2013. Ocular neovascularization. J. Mol. Med. 91, 311–321. https://doi.org/10.1007/s00109-013-0993-5.

Daniel, E., Maguire, M.G., Grunwald, J.E., Toth, C.A., Jaffe, G.J., Martin, D.F., Ying, G.S., 2020. Incidence and progression of nongeographic atrophy in the comparison of age-related macular degeneration treatments trials (catt) clinical trial. JAMA Ophthalmol 138, 510–518. https://doi.org/10.1001/jamaophthalmol.2020.0437.

Eltzschig, H.K., Carmeliet, P., 2011. Hypoxia and inflammation. N. Engl. J. Med. 364, 656–665. https://doi.org/10.1056/NEJMra0910283.

Forooghian, F., Das, B., 2007. Anti-angiogenic effects of ribonucleic acid interference targeting vascular endothelial growth factor and hypoxia-inducible factor-1α. Am. J. Ophthalmol. 144, 761–768. https://doi.org/10.1016/j.ajo.2007.07.022.

Grunwald, J.E., Pistilli, M., Daniel, E., Ying, G.-S., Pan, W., Jaffe, G.J., Toth, C.A., Hagstrom, S.A., Maguire, M.G., Martin, D.F., 2017. Incidence and growth of geographic atrophy during 5 Years of comparison of age-related macular degeneration treatments trials. Ophthalmology 124, 97–104. https://doi.org/10.1016/j.ophtha.2016.09.012.

Grunwald, J.E., Pistilli, M., Ying, G.S., Maguire, M.G., Daniel, E., Martin, D.F., 2015. Growth of geographic atrophy in the comparison of age-related macular degeneration treatments trials. Ophthalmology 122, 809–816. https://doi.org/10.1016/j.ophtha.2014.11.007.

Huang, L.E., Gu, J., Schau, M., Bunn, H.F., 1998. Regulation of hypoxia-inducible factor 1α is mediated by an O2-dependent degradation domain via the ubiquitin-proteasome pathway. Proc. Natl. Acad. Sci. U. S. A 95, 7987–7992. https://doi.org/10.1073/pnas.95.14.7987.

Inoue, Y., Yanagi, Y., Matsuura, K., Takahashi, H., Tamaki, Y., Araie, M., 2007. Expression of hypoxia-inducible factor 1α and 2α in choroidal neovascular membranes associated with age-related macular degeneration. Br. J. Ophthalmol. 91, 1720–1721. https://doi.org/10.1136/bjo.2006.111583.

Ke, Q., Costa, M., 2006. Hypoxia-inducible factor-1 (HIF-1). Mol. Pharmacol. 70, 1469–1480. https://doi.org/10.1124/mol.106.027029.

Kong, D., Park, E.J., Stephen, A.G., Calvani, M., Cardellina, J.H., Monks, A., Fisher, R.J., Shoemaker, R.H., Melillo, G., 2005. Echinomycin, a small-molecule inhibitor of hypoxia-inducible factor-1 DNA-binding activity. Canc. Res. 65, 9047–9055. https://doi.org/10.1158/0008-5472.CAN-05-1235.

Kvanta, A., 2008. Neovascular age-related macular degeneration: too many theories, too little knowledge? Acta Ophthalmol. 86, 468–469. https://doi.org/10.1111/j.1755-3768.2008.01283.x.

Kvanta, A., 2006. Ocular angiogenesis: the role of growth factors. Acta Ophthalmol. Scand. 84, 282–288. https://doi.org/10.1111/j.1600-0420.2006.00659.x.

Kvanta, A., Algvere, P.V., Berglin, L., Seregard, S., 1996. Subfoveal fibrovascular membranes in age-related macular degeneration express vascular endothelial growth factor. Investig. Ophthalmol. Vis. Sci. 37, 1929–1934. https://doi.org/10.1016/s0002-9394(14)70522-7.

Kwon, T.G., Zhao, X., Yang, Q., Li, Y., Ge, C., Zhao, G., Franceschi, R.T., 2011. Physical and functional interactions between Runx 2 and HIF-1α induce vascular endothelial growth factor gene expression. J. Cell. Biochem. 112, 3582–3593. https://doi.org/10.1002/jcb.23289.

Lambert, V., Lecomte, J., Hansen, S., Blacher, S., Gonzalez, M.L.A., Struman, I., Sounni, N.E., Rozet, E., De Tullio, P., Foidart, J.M., Rakic, J.M., Noel, A., 2013. Laser-induced choroidal neovascularization model to study age-related macular degeneration in mice. Nat. Protoc. 8, 2197–2211. https://doi.org/10.1038/nprot.2013.135.

Lin, M., Hu, Y., Chen, Y., Zhou, K.K., Jin, J., Zhu, M., Le, Y.Z., Ge, J., Ma, J.X., 2012. Impacts of hypoxia-inducible factor-1 knockout in the retinal pigment epithelium on

choroidal neovascularization. Investig. Ophthalmol. Vis. Sci. 53, 6197–6206. https://doi.org/10.1167/iovs.11-8936.
Lindekleiv, H., Erke, M.G., 2013. Projected prevalence of age-related macular degeneration in Scandinavia 2012-2040. Acta Ophthalmol. 91, 307–311. https://doi.org/10.1111/j.1755-3768.2012.02399.x.
Locri, F., Dal Monte, M., Aronsson, M., Cammalleri, M., De Rosa, M., Pavone, V., Kvanta, A., Bagnoli, P., André, H., 2019. UPARANT is an effective antiangiogenic agent in a mouse model of rubeosis iridis. J. Mol. Med. 57, 2600–2611. https://doi.org/10.1007/s00109-019-01794-w.
Mammadzada, P., Corredoira, P.M., André, H., 2020. The role of hypoxia-inducible factors in neovascular age-related macular degeneration: a gene therapy perspective. Cell. Mol. Life Sci. 77, 819–833. https://doi.org/10.1007/s00018-019-03422-9.
Mammadzada, P., Gudmundsson, J., Kvanta, A., André, H., 2016. Differential hypoxic response of human choroidal and retinal endothelial cells proposes tissue heterogeneity of ocular angiogenesis. Acta Ophthalmol. 94, 805–814. https://doi.org/10.1111/aos.13119.
Martin, D.F., Maguire, M.G., Fine, S.L., Ying, G.S., Jaffe, G.J., Grunwald, J.E., Toth, C., Redford, M., Ferris, F.L., 2012. Ranibizumab and bevacizumab for treatment of neovascular age-related macular degeneration: two-year results. Ophthalmology 119, 1388–1398. https://doi.org/10.1016/j.ophtha.2012.03.053.
McCullough, S., Milesi-Halle, A., Hinson, J.A., Kurten, R.C., Lamps, L.W., Brown, A., James, L.P., 2013. Echinomycin decreases iduction of VEGF and hepatocyte regeneration in acetminophen overdose. Pharmacol Toxicol Basic Clin 16, 387–393. https://doi.org/10.1016/j.cmet.2012.08.002.
Miller, J.W., 2013. Age-related macular degeneration revisited - piecing the puzzle: the LXIX edward jackson memorial lecture. Am. J. Ophthalmol. 155, 1–35. https://doi.org/10.1016/j.ajo.2012.10.018 e13.
Nagai, N., Suzuki, M., Uchida, A., Kurihara, T., Kamoshita, M., Minami, S., Shinoda, H., Tsubota, K., Ozawa, Y., 2016. Non-responsiveness to intravitreal aflibercept treatment in neovascular age-related macular degeneration: implications of serous pigment epithelial detachment. Sci. Rep. 6, 1–10. https://doi.org/10.1038/srep29619.
Otsuji, T., Nagai, Y., Sho, K., Tsumura, A., Koike, N., Tsuda, M., Nishimura, T., Takahashi, K., 2013. Initial non-responders to ranibizumabin the treatment of age-related macular degeneration (AMD). Clin. Ophthalmol. 7, 1487–1490. https://doi.org/10.2147/OPTH.S46317.
Ruas, J.L., Poellinger, L., 2005. Hypoxia-dependent activation of HIF into a transcriptional regulator. Semin. Cell Dev. Biol. 16, 514–522. https://doi.org/10.1016/j.semcdb.2005.04.001.
Semenza, G.L., 2011. Oxygen sensing, homeostasis, and disease. N. Engl. J. Med. 365, 537–547. https://doi.org/10.1056/NEJMra1011165.
Semenza, G.L., 2007. Hypoxia-inducible factor 1 (HIF-1) pathway. Sci. STKE. https://doi.org/10.1126/stke.4072007cm8, 2007.
Sheridan, C.M., Pate, S., Hiscott, P., Wong, D., Pattwell, D.M., Kent, D., 2009. Expression of hypoxia-inducible factor-1α and -2α in human choroidal neovascular membranes. Graefe's Arch. Clin. Exp. Ophthalmol. 247, 1361–1367. https://doi.org/10.1007/s00417-009-1133-3.
Shin, J.M., Kim, J., Kim, H.E., Lee, M.J., Lee, K. Il, Gyong Yoo, E., Joo Jeon, Y., , Chae, D. W.K.J. Il, Chung, H.M., 2011. Enhancement of differentiation efficiency of hESCs into vascular lineage cells in hypoxia via a paracrine mechanism. Stem Cell Res. 7, 173–185. https://doi.org/10.1016/j.scr.2011.06.002.
Smith, R.O., Ninchoji, T., Gordon, E., André, H., Dejana, E., Vestweber, D., Kvanta, A., Claesson-Welsh, L., 2020. Vascular permeability in retinopathy is regulated by VEGFR2 Y949 signaling to VE-cadherin. Elife 9, e54056. https://doi.org/10.7554/eLife.54056.
Takei, A., Ekström, M., Mammadzada, P., Aronsson, M., Yu, M., Kvanta, A., André, H., 2017. Gene transfer of prolyl hydroxylase domain 2 inhibits hypoxia-inducible angiogenesis in a model of choroidal neovascularization. Sci. Rep. 7, 1–14. https://doi.org/10.1038/srep42546.
Tsuzuki, T., Okada, H., Shindoh, H., Shimoi, K., Nishigaki, A., Kanzaki, H., 2016. Effects of the hypoxia-inducible factor-1 inhibitor echinomycin on vascular endothelial growth factor production and apoptosis in human ectopic endometriotic stromal cells. Gynecol. Endocrinol. 32, 323–328. https://doi.org/10.3109/09513590.2015.1121225.
Vadlapatla, R., Vadlapudi, A., Mitra, A., 2013. Hypoxia-inducible factor-1 (HIF-1): a potential target for intervention in ocular neovascular diseases. Curr. Drug Targets 14, 919–935. https://doi.org/10.2174/13894501113149990015.
Wang, G.L., Jiang, B.H., Rue, E.A., Semenza, G.L., 1995. Hypoxia-inducible factor 1 is a basic-helix-loop-helix-PAS heterodimer regulated by cellular O2 tension. Proc. Natl. Acad. Sci. Unit. States Am. 92, 5510–5514. https://doi.org/10.1073/pnas.92.12.5510.
Wang, G.L., Semenza, G.L., 1995. Purification and characterization of hypoxia-inducible factor 1. J. Biol. Chem. 270, 1230–1237. https://doi.org/10.1074/jbc.270.3.1230.
Weidemann, A., Johnson, R.S., 2008. Biology of HIF-1α. Cell Death Differ. 15, 621–627. https://doi.org/10.1038/cdd.2008.12.
Wong, W.L., Su, X., Li, X., Cheung, C.M.G., Klein, R., Cheng, C.Y., Wong, T.Y., 2014. Global prevalence of age-related macular degeneration and disease burden projection for 2020 and 2040: a systematic review and meta-analysis. Lancet Glob. Heal. 2, 106–116. https://doi.org/10.1016/S2214-109X(13)70145-1.
Yamaguchi, J., Tanaka, T., Saito, H., Nomura, S., Aburatani, H., Waki, H., Kadowaki, T., Nangaku, M., 2017. Echinomycin inhibits adipogenesis in 3T3-L1 cells in a HIF-independent manner. Sci. Rep. 7, 6516. https://doi.org/10.1038/s41598-017-06761-4.
Yao, Y., Wang, L., Zhou, J., Zhang, X., 2017. HIF-1α inhibitor echinomycin reduces acute graft-versus-host disease and preserves graft-versus-leukemia effect. J. Transl. Med. 15, 1–11. https://doi.org/10.1186/s12967-017-1132-9.
Zudaire, E., Gambardella, L., Kurcz, C., Vermeren, S., 2011. A computational tool for quantitative analysis of vascular networks. PloS One 6, 1–12. https://doi.org/10.1371/journal.pone.0027385.